

Hierarchical Self-Assembly of GaAs/AlGaAs Quantum Dots

A. Rastelli,^{1,*} S. Stuffer,² A. Schliwa,³ R. Songmuang,¹ C. Manzano,¹ G. Costantini,¹ K. Kern,¹ A. Zrenner,² D. Bimberg,³ and O. G. Schmidt¹

¹Max-Planck-Institut für Festkörperforschung, Heisenbergstrasse 1, D-70569 Stuttgart, Germany

²Experimentalphysik, Universität Paderborn, Warburgerstrasse 100, D-33098 Paderborn, Germany

³Institut für Festkörperphysik, Technische Universität Berlin, PN 5-2, Hardenbergstrasse 36, D-10623 Berlin, Germany

(Received 17 September 2003; published 21 April 2004)

A novel structure containing *self-assembled*, unstrained GaAs quantum dots is obtained by combining solid-source molecular beam epitaxy and atomic-layer precise *in situ* etching. Photoluminescence (PL) spectroscopy reveals light emission with very narrow inhomogeneous broadening and clearly resolved excited states at high excitation intensity. The dot morphology is determined by scanning probe microscopy and, combined with single band and eight-band $k \cdot p$ theory calculations, is used to interpret PL and single-dot spectra with no adjustable structural parameter.

DOI: 10.1103/PhysRevLett.92.166104

PACS numbers: 68.65.Hb, 68.47.Fg, 78.55.Cr, 78.67.Hc

Semiconductor quantum dots (QDs) are attracting much interest because of their application in novel optoelectronic devices and systems [1–3]. The most convenient method to produce QDs is the Stranski-Krastanow (SK) growth mode, in which defect-free three-dimensional (3D) islands spontaneously form on top of a thin wetting layer (WL) during lattice-mismatched heteroepitaxial growth. SK-grown QDs are strained and significant intermixing usually occurs both during island formation [4] and overgrowth [5], rendering QD geometry and composition uncertain.

GaAs/AlGaAs QDs cannot be created by SK growth because of the almost perfect match of lattice parameters. Nevertheless, this system offers several advantages compared to others: The grown material is ideally unstrained, and sharp interfaces with reduced intermixing can be obtained; AlGaAs heterostructures have been intensively studied [6] and can be designed to emit light in the optimum spectral range of the most advanced optical components available nowadays. For these reasons, GaAs QDs naturally occurring at thickness fluctuations of thin GaAs/AlGaAs quantum wells (QWs) have been used as a model to study fundamental properties of QDs [7–11] and coherent optical manipulation of QD states [12–15]. However, such QDs have small confinement energy $E_c \approx 10$ meV, and their geometry is poorly known. Self-assembled 3D QDs with larger E_c have been grown by modified-droplet epitaxy [16]. However, this technique requires growth at low temperatures and the obtained QDs show poor size homogeneity. Because of their appeal, GaAs QDs have also been fabricated by means of several more elaborate methods requiring substrate pre-patterning, postgrowth processing, etc., (see, e.g., Ref. [17], and references therein).

In this Letter we present a simple method to obtain 3D GaAs/AlGaAs QDs via multistep (*hierarchical*) self-assembly. First we create a template of SK-grown InAs/GaAs(001) islands, which are “converted” into nanoholes on a GaAs surface by GaAs overgrowth followed by

in situ etching [18]. Self-assembled nanoholes are then transferred to an AlGaAs surface, filled with GaAs, and overgrown with AlGaAs. Because of the absence of sizable intermixing, the QD morphology is given by the shape of the AlGaAs nanoholes, which we determine by scanning tunneling microscopy (STM) and atomic force microscopy (AFM). The good size homogeneity of the QDs results in a photoluminescence (PL) linewidth as narrow as 11 meV. This allows us to observe excited states as well as a redshift of the ground-state emission at high excitation intensity for a large ensemble of QDs. The latter observation is due to multiexcitonic effects, which we confirm by single-QD PL spectroscopy. Nominal compositions and measured geometry are used as input to single band and eight-band $k \cdot p$ theory calculations. In contrast to SK-grown QDs, where assumptions on QD structure are necessary, our calculations enable us to interpret the main features of the PL spectra with no adjustable structural parameter.

The samples used for this study are grown on GaAs(001) substrates by a solid-source molecular beam epitaxy system equipped with an AsBr₃ etching unit [18,19]. The characterization of the surface morphology is performed by AFM and, in ultrahigh vacuum (UHV), by room-temperature STM. The optical properties of the structures are investigated by standard PL spectroscopy. For selected samples we also perform single-QD PL and PL excitation (PLE) spectroscopy measurements by focusing the laser on the sample through a low-temperature microscope with high numerical aperture.

The sample preparation begins with the substrate de-oxidation, followed by the growth of a 340-nm thick GaAs buffer at a rate of 0.6 monolayer/s (ML/s). An ensemble of large InAs/GaAs islands with narrow size distribution is then obtained by growing InAs at a growth rate of 0.01 ML/s and a substrate temperature $T_s = 500$ °C. The InAs islands are overgrown with 10-nm GaAs and then etched for nominal 5 nm by AsBr₃ gas. Strain-enhanced etching results in the preferential

removal of the buried InAs islands and in the *spontaneous* formation of nanoholes at their place [18,19]. Subsequently, we deposit a layer of $\text{Al}_{0.45}\text{Ga}_{0.55}\text{As}$ with thickness D on the GaAs surface with nanoholes. Because of the low surface diffusivity of Al at T_s , we expect the GaAs surface nanoholes to be transferred to the AlGaAs surface. This is confirmed by the AFM images shown in Figs. 1(a) and 1(b). By performing a statistical analysis on the hole morphology as a function of D we find that the average hole depth decreases as the AlGaAs overgrowth proceeds [Fig. 1(c)]. At the same time, holes shrink in the $[1\bar{1}0]$ direction while their size in the $[110]$ direction remains approximately unchanged [Fig. 1(d)]. This is most probably due to the anisotropy in surface diffusivity of Al and Ga [20]: Since the diffusivity along the $[1\bar{1}0]$ direction is higher than along the $[110]$, holes tend to fill first in the former direction.

In order to produce QDs, the AlGaAs holes need to be filled with GaAs. This is done by overgrowing the holes with a $d = 2$ -nm thick GaAs layer at T_s and by annealing the sample for 2 min at T_s . This results in the spontaneous recovery of an atomically flat surface. A 100-nm thick $\text{Al}_{0.35}\text{Ga}_{0.65}\text{As}$ barrier, a 20-nm thick $\text{Al}_{0.45}\text{Ga}_{0.55}\text{As}$ cladding layer, and a 10-nm thick GaAs cap complete the structure [Fig. 2(a)]. With this layer choice, we obtain “inverted” GaAs/AlGaAs QDs below a thin QW [see magnification in Fig. 2(a)]. The QW thickness d_{QW} can be estimated as $d_{\text{QW}} \approx d - V_{\text{holes}}/u$, where V_{holes} is the total volume of GaAs necessary to fill the holes contained

in a surface of unit area u . (V_{holes} can be obtained from the AFM data.) The QD size and shape are fully determined by the size and shape of the holes on the $\text{Al}_{0.45}\text{Ga}_{0.55}\text{As}$ surface. Therefore, a simple way to tune the QD size is to vary D [see Figs. 1(c) and 1(d)]. Other possibilities include changing the initial GaAs hole morphology (by tuning the InAs island size, varying the etching time, or etching a stack of several layers of InAs islands [21]) or varying the AlGaAs growth temperature and/or Al content. The optical properties of the structure shown in Fig. 2(a) are studied by PL spectroscopy, as a function of D . Figure 2(b) shows a series of low excitation intensity ($I_{\text{exc}} = 1.5 \text{ W/cm}^2$) spectra collected at 8 K for samples with D varying between 5 and 20 nm. The bottom spectrum corresponds to a reference 2-nm thick $\text{Al}_{0.45}\text{Ga}_{0.55}\text{As}/\text{GaAs}/\text{Al}_{0.35}\text{Ga}_{0.65}\text{As}$ QW without QDs. We assign the peak at energy $E_{\text{QW}} = 1.777 \text{ eV}$ to the bound-exciton recombination in the asymmetric QW. The broad emission is mainly due to the roughness of the inverted $\text{Al}_{0.45}\text{Ga}_{0.55}\text{As}/\text{GaAs}$ interface.

When nanoholes are present on the $\text{Al}_{0.45}\text{Ga}_{0.55}\text{As}$ surface prior to GaAs overgrowth, a second peak appears at an energy E^0 which clearly depends on D . We assign this peak to carrier recombination inside the QDs. With increasing D , E^0 shows a pronounced blueshift, while E_{QW} [22] slightly redshifts [Fig. 2(c)]. We ascribe this behavior to a reduction of the average hole depth $\langle h \rangle$ and a consequent increase of the QW thickness d_{QW} . Remarkably, the sample with $D = 5$ displays an ultranarrow QD emission line with FWHM of 11 meV. We achieved even

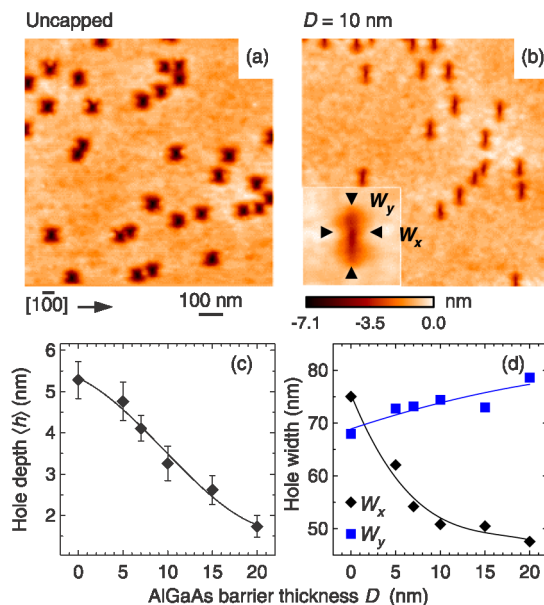


FIG. 1 (color online). AFM images of GaAs nanoholes prior to (a) and after (b) overgrowth with $D = 10$ nm of $\text{Al}_{0.45}\text{Ga}_{0.55}\text{As}$. The inset of (b) shows a $150 \times 150 \text{ nm}^2$ magnification of a nanohole with widths W_x and W_y in the $[1\bar{1}0]$ and $[110]$ directions, respectively. (c) Average depth $\langle h \rangle$ and (d) widths of holes as a function of D . Error bars in (c) represent standard deviations.

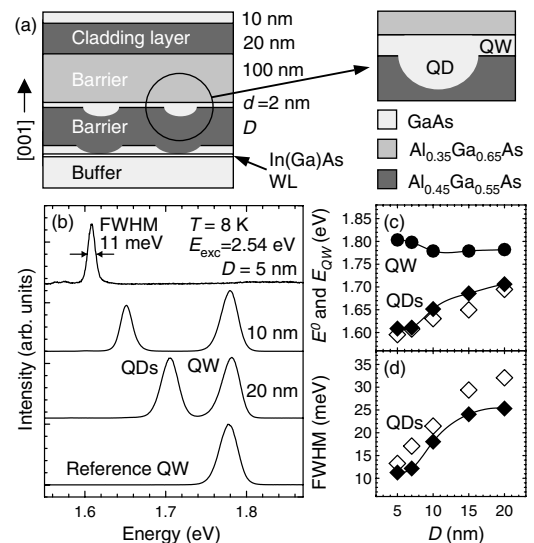


FIG. 2. (a) Schematic sample structure and magnification of the active layer. (b) Low excitation PL spectra of samples with different AlGaAs-barrier thickness D . Measurement temperature T and laser excitation energy E_{exc} are indicated. (c) Positions of the peaks associated with GaAs QDs (E^0) and with the GaAs QW (E_{QW}) and (d) FWHM of the QD peak as a function of D . Open symbols refer to the result of a 1D simulation (see the text).

FWHM = 8.9 meV by etching a stack of two layers of InAs islands [21]. In addition, large confinement energies $E_c = E_{QW} - E^0 \approx 200$ meV or more can be obtained with this method [see Figs. 2(b) and 2(c)]. The QD emission broadens with increasing D [Fig. 2(d)], because of a broadening of the relative hole-depth distribution [see Fig. 1(c)].

Our interpretation is supported by a simple calculation within the effective mass approximation with material parameters taken from Ref. [6]. Since our QDs are rather shallow (see Fig. 1) the ground-state transition energy E_i^0 of the i th QD is mainly determined by its vertical size, given by $h_i + d_{QW}$, where h_i is the depth of the corresponding hole. The monodimensional (1D) Schrödinger equation with the Ben Daniel–Duke Hamiltonian [23] is solved for electrons and heavy holes in the Γ valley. Single particle energy levels are calculated for a large number of QDs with h_i and d_{QW} extracted from the AFM data. The PL spectra are then simulated by histogramming the E_i^0 's. We thus determine peak positions E^0 and FWHM as a function of D as shown with open symbols in Figs. 2(c) and 2(d). In spite of the simplifying assumptions, the experimental trends are well reproduced.

A distinctive feature to be expected for QDs is a state filling effect and the appearance of excited states as I_{exc} is increased (see, e.g., Refs. [10,24]). This is what we observe in Fig. 3 for a sample with $D = 7$ nm. At least four excited states in the energy range from E^0 to E_{QW} are visible, and even more appear at higher I_{exc} (not shown). A similar behavior is observed for other samples with very narrow inhomogeneous broadening, such as that with $D = 5$ nm. For samples with $D \geq 10$ nm, the peak at E^0 shows only a broadening on the high-energy side, as I_{exc} is increased.

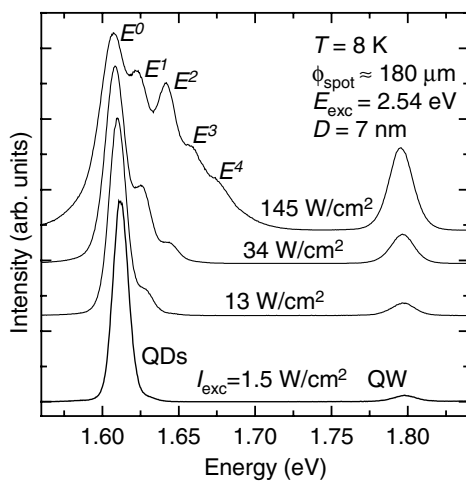


FIG. 3. PL spectra for a sample with $D = 7$ nm for various excitation intensities I_{exc} . When I_{exc} is increased, well defined excited states E^1 , E^2 , E^3 , and E^4 appear while the peak E^0 slightly redshifts. The laser spot diameter ϕ_{spot} is also indicated.

A subtle effect noticeable in Fig. 3 with increasing I_{exc} is a monotonic redshift of the E^0 peak. The total shift measured by varying I_{exc} from 1.5 to 145 W/cm² is 3.7 meV. In order to understand this behavior and to gather further insight in the optical properties of our QDs, we performed single-QD PL and PLE spectroscopy measurements [Fig. 4(a)] on a sample containing QDs with very low surface density ($0.5 \mu\text{m}^{-2}$). The spectra show narrow lines, with widths limited by the measurement resolution (about 200 μeV), witnessing the high quality of the structure. At low excitation [spectrum PL1 in Fig. 4(a)] the single line is due to ground-state excitons (X) confined in the QD. At higher I_{exc} [spectra PL2 and PL3 in Fig. 4(a)], peaks appear at the low-energy side of X . We identify a biexcitonic line (XX) [8] separated by 3.0 meV from the X line and probable multiexcitonic lines [25]. In spectrum PL3 such lines become more intense than the X line and are responsible for the redshift of the E^0 peak in Fig. 3. Spectra PL2 and PL3 show features also on the high-energy side of X . At very high I_{exc} (spectrum PL3) many lines evolve and merge into broad peaks similar to those observed in Fig. 3, most probably because a large number of carriers populates the investigated QD and its surroundings. For this reason we focus

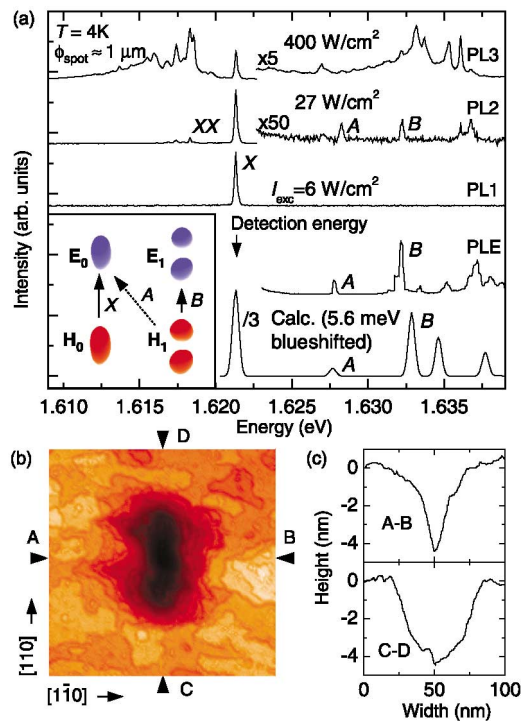


FIG. 4 (color online). (a) PL ($E_{exc} = 1.96$ eV) and PLE spectra of a single QD with $D = 7$ nm for different I_{exc} . The bottom graph is a calculated excitonic absorption spectrum and the inset shows 3D representations of ground and first excited state wave functions for electrons (E) and holes (H) in the QD. (b) STM topograph, with contrast enhanced by a first derivative filtering, taken at constant current (0.2 nA) and sample bias (-4.2 V), of the AlGaAs nanohole ($D = 7$ nm) used for the calculation shown in (a). (c) Line scans of the STM image.

our attention on the few peaks appearing at moderate excitation (spectrum PL2). Some of them (e.g., those labeled with *A* and *B*) can be attributed to a recombination of excited-state excitons. This is confirmed by the PLE spectrum shown in Fig. 4(a) obtained by scanning the excitation energy E_{exc} and detecting the light emission at the *X* energy. Similar spectra were obtained for several other QDs in the same sample confirming the good ensemble homogeneity.

Thanks to the negligible intermixing and absence of strain, we can aim to calculate the optical properties of our QDs by taking as input nominal layer compositions and measured QD geometry. To exclude influences of the surface oxide, we determined the hole morphology at high resolution by UHV STM. Figures 4(b) and 4(c) show an STM image of a typical nanohole after overgrowth with $D = 7$ nm of $\text{Al}_{0.45}\text{Ga}_{0.55}\text{As}$ and corresponding line scans along the $[1\bar{1}0]$ (A-B) and $[110]$ (C-D) directions. With the hole geometry given by STM and a QW thickness of 2 nm [see Fig. 2(a)], we calculate the excitonic absorption spectrum of such a GaAs QD by using eight-band $k \cdot p$ theory (see Refs. [26,27] for details). The calculated spectrum, shown in Fig. 4(a), is blueshifted 5.6 meV so that the energy of the ground-state transition matches the measured one. We have no access to the exact geometry of the QD measured by PL, but the shift is well within the FWHM (12 meV) of the inhomogeneously broadened E^0 peak for this sample. We see that the position of the peaks *A* and *B* is well reproduced by the calculation. In a single particle picture, with electron and hole levels labeled E_j and H_j , respectively, these two absorption lines originate from the H_1-E_0 and H_1-E_1 transitions, as depicted in the inset of Fig. 4(a). Since the overlap integral of wave functions with different index j is small [see the representation of the envelope wave functions in the inset of Fig. 4(a)] the calculated *A* peak is less intense than the *B* peak. This result is in good agreement with the experimental PLE spectrum shown in Fig. 4(a). To our knowledge, this is the first direct comparison of a calculated absorption spectrum with no adjustable structural parameters to measured single-QD PL and PLE spectra.

In conclusion, we have combined SK growth and *in situ* etching to produce *self-assembled*, unstrained, inverted GaAs QDs with tunable size, large confinement energy, and good size homogeneity. Since the QD positions are determined by those of the InAs template, the QD density can be controlled, and laterally coupled GaAs QDs could possibly be grown by using InAs QD molecules [18] as a template. Moreover, our QDs have transition energies in the optimum working range of Si photodetectors and short-pulse Ti:sapphire lasers, commonly used for coherent optical experiments. Thus, the presented *self-assembled* QDs are preferable both to 3D In(Ga)As/GaAs QDs [28] and to shallow QDs in thin GaAs/AlGaAs QWs [7–15], and can be used as a new playground for investigating the possibilities of using

QDs as building blocks for quantum information processing.

M. Saraydarov, L. C. Andreani, and S. Kiravittaya are acknowledged for fruitful discussions and K. v. Klitzing for his interest and support. This work was supported by the BMBF (01BM906/4). A. S. and D. B. thank the Sfb 296.

*Electronic address: A.Rastelli@fkf.mpg.de

- [1] Z. Yuan *et al.*, *Science* **295**, 102 (2002).
- [2] D. Bimberg and N. N. Ledentsov, *J. Phys. Condens. Matter* **15**, R1063 (2003).
- [3] A. Zrenner, *J. Chem. Phys.* **112**, 7790 (2000).
- [4] I. Kegel *et al.*, *Phys. Rev. Lett.* **85**, 1694 (2000); F. Boscherini *et al.*, *Appl. Phys. Lett.* **76**, 682 (2000); U. Denker, M. Stoffel, and O. G. Schmidt, *Phys. Rev. Lett.* **90**, 196102 (2003).
- [5] P. B. Joyce *et al.*, *Surf. Sci.* **492**, 345 (2001); A. Rastelli, M. Kummer, and H. von Känel, *Phys. Rev. Lett.* **87**, 256101 (2001).
- [6] *Properties of Aluminium Gallium Arsenide*, Data Review Series Vol. 7, edited by S. Adachi (The Institute of Electrical Engineers, London, 1993).
- [7] J. Christen and D. Bimberg, *Phys. Rev. B* **42**, 7213 (1990).
- [8] K. Brunner *et al.*, *Phys. Rev. Lett.* **73**, 1138 (1994).
- [9] A. Zrenner *et al.*, *Phys. Rev. Lett.* **72**, 3382 (1994).
- [10] D. Gammon *et al.*, *Phys. Rev. Lett.* **76**, 3005 (1996).
- [11] K. Matsuda *et al.*, *Phys. Rev. Lett.* **91**, 177401 (2003).
- [12] T. H. Stievater *et al.*, *Phys. Rev. Lett.* **87**, 133603 (2001).
- [13] A. Zrenner *et al.*, *Nature (London)* **418**, 612 (2002).
- [14] X. Li *et al.*, *Science* **301**, 809 (2003).
- [15] J. Hours *et al.*, *Appl. Phys. Lett.* **82**, 2206 (2003).
- [16] K. Wanatabe, N. Koguchi, and Y. Gotoh, *Jpn. J. Appl. Phys.* **39**, L79 (2000).
- [17] A. Hartmann *et al.*, *Appl. Phys. Lett.* **73**, 2322 (1998).
- [18] R. Songmuang, S. Kiravittaya, and O. G. Schmidt, *Appl. Phys. Lett.* **82**, 2892 (2003).
- [19] H. Schuler, N. Y. Jin-Phillipp, F. Phillipp, and K. Eberl, *Semicond. Sci. Technol.* **13**, 1341 (1998).
- [20] K. Shiraishi, *Appl. Phys. Lett.* **60**, 1363 (1992).
- [21] A systematic study will be published.
- [22] For the sample with $D = 5$ nm the QW peak is visible only at higher I_{exc} .
- [23] M. A. Herman, D. Bimberg, and J. Christen, *J. Appl. Phys.* **70**, R1 (1991).
- [24] H. Lipsanen, M. Sopanen, and J. Ahopelto, *Phys. Rev. B* **51**, 13 868 (1995).
- [25] F. Findeis, A. Zrenner, G. Böhm, and G. Abstreiter, *Solid State Commun.* **114**, 227 (2000).
- [26] O. Stier, M. Grundmann, and D. Bimberg, *Phys. Rev. B* **59**, 5688 (1999).
- [27] D. Bimberg, M. Grundmann, and N. N. Ledentsov, *Quantum Dot Heterostructures* (John Wiley & Sons, Chichester, 1998); V. A. Shchukin, N. N. Ledentsov, and D. Bimberg, *Epitaxy of Nanostructures*, Nanoscience and Technology Series (Springer, New York, 2004).
- [28] H. Htoon *et al.*, *Phys. Rev. Lett.* **88**, 087401 (2002); P. Borri *et al.*, *Phys. Rev. B* **66**, 081306 (2002).